ELSEVIER

Microelectronics Reliability 44 (2004) 621–626

MICROELECTRONICS RELIABILITY

www.elsevier.com/locate/microrel

# Numerical analysis of the warpage problem in TSOP

Kyoungsoon Cho [a], Insu Jeon [b,*]

[a] *EMC Memory Research Team, Kumgang Korea Chemical Co., Ltd., 85, Mabook-ri, Koosung-eub, Youngin-si, Kyoungki-do 449-910, South Korea*

[b] *PKG & Module R&D Center, Hynix Semiconductor Inc., San 136-1, Ami-ri, Bubal-eub, Ichon-si, Kyoungki-do 467-791, South Korea*

Received 16 May 2003; received in revised form 9 December 2003

## Abstract

The reliability and the solderability of thin small outline package (TSOP) are significantly affected by the warpage that is generated after epoxy molding compound (EMC) molding process. This warpage problem mainly results from the mismatch of material properties such as Young's modulus, Poisson's ratio and coefficient of thermal expansion (CTE) and the geometric structure of each component for TSOP. The optimization of both material properties and geometric structures using the numerical analysis is necessary to reduce the warpage of TSOP. However, there are still some limitations for the numerical analysis to obtain proper results consistent with the practical warpage values. In this paper, the numerical analysis is performed under the assumption of elastic behavior for EMC. Furthermore, to solve the limitations, the material properties at the molding temperature and the degree of reaction rate at the end of the molding process of EMC are considered together for the analysis. This numerical analysis gives the higher warpage values than the measured ones, and is applicable to the practical design of the reliable electronic package.

## 1. Introduction

As thin small outline package (TSOP) becomes thinner and smaller with its design rule, the warpage of TSOP becomes more and more important. The warpage that is generated after epoxy molding compound (EMC) molding process has a great effect on the workability of the backend process such as the trim forming and the soldering. Also, it is an important factor in the reliability problems such as the chip crack, i.e., the intermetallic dielectric (IMD) crack and the package crack problems. Therefore, the numerical analysis for predicting and analyzing the warpage of TSOP is very important to fabricate the reliable TSOP products.

However, the numerical analysis has still some limitations to obtain proper results consistent with the practical warpage. Under the assumption of elastic behavior for EMC, the warpage analysis for TSOP has been often carried out because of its simplicity and convenience for the computation [1–3]. The analysis with this assumption, however, hardly gives a good agreement between the computed warpage results and the experimentally measured ones because the temperature dependence of the material properties cannot be considered for the analysis.

Recently, the numerical analysis under the assumption of viscoelastic behavior for EMC that can theoretically characterize the material properties depending on the temperature and the time, has been executed for improving the weak points of the consideration of elastic behavior for EMC [4–6]. This assumption, however, has many ambiguities in mathematical modeling of the actual viscoelastic behavior of EMC and also has many difficulties in measuring the absolute magnitude of material properties. Therefore, the analysis with the consideration of elastic behavior for EMC, which is also including the temperature effect on the material properties, is essential to solve the limitations.

In this paper, the numerical analysis of the warpage problem in TSOP is carried out under the assumption of

---

[*] Corresponding author. Present address: Department of Mechanical and Control Engineering, Tokyo Institute of Technology, 2-12-1 O-okayama, Meguro-ku, Tokyo 152-8552, Japan. Tel.: +81-3-5734-2783; fax: +81-3-5734-3917.

*E-mail address:* i_jeon@mep.titech.ac.jp (I. Jeon).

0026-2714/$ - see front matter © 2004 Elsevier Ltd. All rights reserved.
doi:10.1016/j.microrel.2003.12.009

elastic behavior for EMC considering the three main particulars as follows. Firstly, the selection of the reasonable material properties of EMC is discussed for the analysis. Secondly, when the test specimens are fabricated for measuring the material properties of EMC, the actual molding process condition is taken into account. Finally, the automatic measurement system, NEXIV VMR-6555, is used for accurate measurement of the practical warpage of TSOP.

## 2. Model review

The assumption of elastic or elastic–plastic behavior for the inorganic components of TSOP such as DRAM chip and lead frame is adequate for numerical analysis. For the organic component such as EMC, however, the assumption of elastic behavior is not suitable for the analysis because the elastic modulus of EMC increases about 15–20 times with the cooling down process from the molding temperature to the room temperature.

A simple example is prepared to explain the reason of this problem. Consider an elastic bar constrained by the rigid wall, which is shown in Fig. 1. When the temperature is cooling down from $T_1 = 125$ °C to $T_2 = 25$ °C, the thermal stress can be calculated with $\sigma = -E\alpha\Delta T$, where $E$ is elastic modulus, $\alpha$ is coefficient of thermal expansion (CTE) and $\Delta T$ is temperature difference. If elastic modulus is assumed to be changed according to the temperature change, for instance, from $E_{T=25\,^{\circ}\mathrm{C}} =$ 100 GPa to $E_{T=125\,^{\circ}\mathrm{C}} = 1$ GPa (see the dotted curve in Fig. 2), and CTE is assumed to be constant as $\alpha =$ 10 ppm/°C, the thermal stress of this example comes to 100 MPa because the thermal stress is calculated using only the elastic modulus of the final temperature state. The exact thermal stress of this example, on the other hand, can be calculated with the consideration of the entire change of the elastic modulus following the change of the temperature.

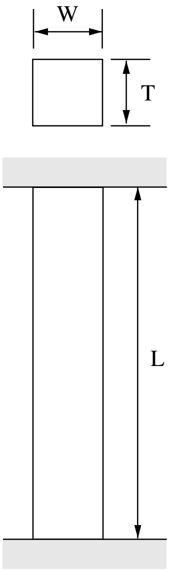

Fig. 1. A constrained bar to calculate the thermal stress.

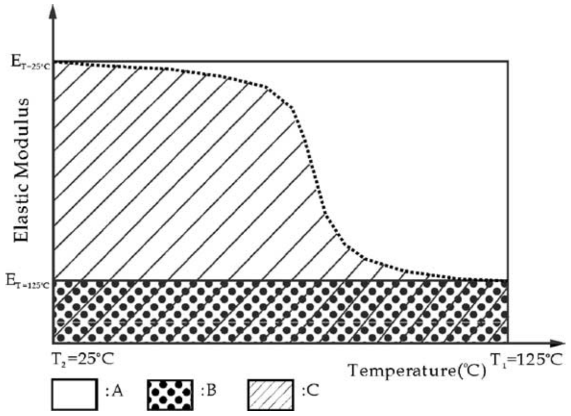

Fig. 2. The change of the elastic modulus with the change of the temperature.

The difference between these two calculations for the thermal stress is graphically shown in Fig. 2. The thermal stress under the assumption of elastic behavior of EMC caused by the cooling down process can be calculated from ($A$ area) × $\alpha$. The exact thermal stress of this example can be calculated from ($C$ area) × $\alpha$ if the time–temperature relation of the material property is ignored. Therefore, the calculated exact stress value is lower than the stress that is calculated during the cooling down process and the exact thermal stress of this example always stays between ($A$ area) × $\alpha$ and ($B$ area) × $\alpha$.

The warpage problem of this study is the same example as the one for calculating the thermal stress. The actual warpage values also stay between the computed warpage values using the material data at the molding temperature and at the room temperature. This is the reason for the difference between the computed warpage results and the measured ones. Moreover, the warpage values calculated with the material data at the molding temperature are always higher than that calculated with the material data at the room temperature [7]. Thus we exploit the material properties at the molding temperature for numerical analysis to obtain the overestimated warpage values comparing with the actual warpage ones.

## 3. Thermo-mechanical characteristics of EMC

EMC is generally made up with epoxy and phenolic resins, and the cure reaction progresses with following three steps; firstly, raw materials are mixed and kneaded in the melt state, in this step the degree of reaction rate goes up to 20–30%. Secondly, EMC is molded and the reaction rate in this step reaches about 85%. Then complete reaction is achieved through post-mold cure (PMC) process. The material properties of EMC, such as elastic modulus, CTE, and glass transition ($T_g$) are mainly determined in the reaction step.

Particularly, for the elastic modulus of EMC, the 3-point bending test has been performed using the universal testing machine (LLOYD, LR-10K). Moreover, three types of specimens are prepared with respect to the degrees of reaction rate, 85%, 90%, and 100%. Fig. 3(a) and (b) shows the measured results of elastic modulus, $T_g$ and CTE. It is found that elastic modulus and $T_g$ are increased with the increase of the degree of reaction rate and CTE is almost unchanged with the change of the degree of reaction rate.

To attain the same degree of reaction rate for the test specimen to the level of actual molding process, the cure time of the specimen has to be decided. The degree of reaction rate, 85%, in actual molding condition at 185 °C is calculated from the thermal analysis by different scanning calorimeter (DSC). The isothermal degree of reaction rate for the cure time is generally decided by the isothermal method. However, this method has some difficulties to insure the temperature stability. The isothermal degree of reaction rate is, therefore, often calculated by the dynamic method in indirect way. In this study, the dynamic method is applied for the isothermal data. The temperature increasing rate is chosen as 10 °C/min from 25 to 250 °C, and the obtained dynamic data is converted to the isothermal data by the $n$th order cure kinetics (B & D kinetics) [8] equation given as

$$\frac{d\alpha}{dt} = k(1-\alpha)^n \qquad (1)$$

where $k = k_0 \exp(-E_a/RT)$, $n$ is the reaction order, $k_0$ is Arrhenius frequency factor and $E_a$ is activation energy, respectively.

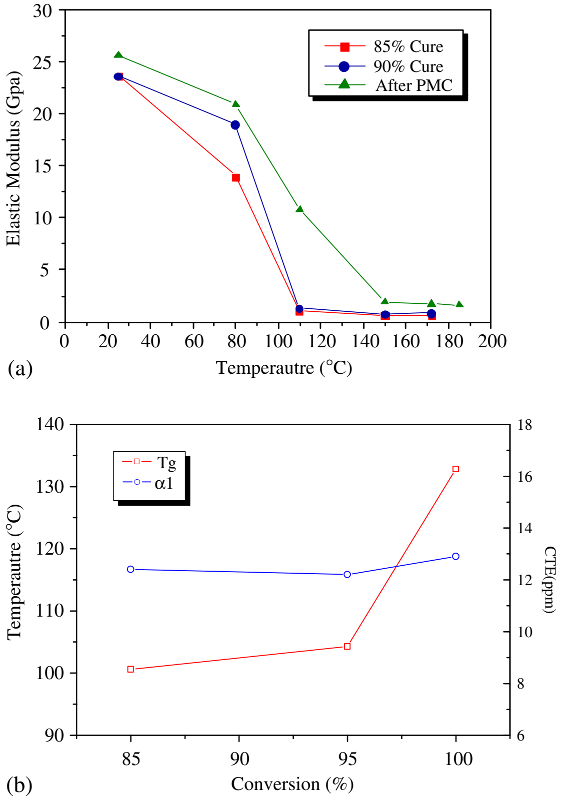

Fig. 3. (a) The elastic modulus and (b) $T_g$ and $\alpha_1$ depending on the temperature and the degree of reaction rate of EMC.

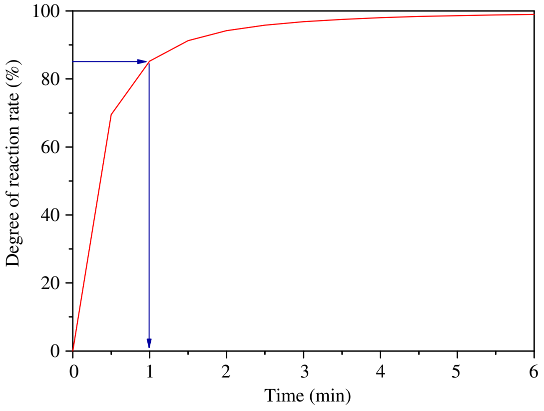

Fig. 4. The isothermal degree of reaction rate of EMC.

Fig. 4 shows the isothermal data obtained by integrating the $n$th order cure kinetics equation. It is found that the cure time is 60 s, when the degree of reaction rate for the test specimen reaches to 85%.

## 4. Finite element analysis for the warpage in TSOP

TSOP Type I and TSOP Type II for 256 M SDRAM, which have different structures of the lead frame with each other, are selected for this study. For the simplicity of the computation, only a quarter part of the total package is considered. The mesh configuration of TSOP Type I after molding process and its boundary condition are shown in Fig. 5. The package code ABAQUS is employed for the finite element solution, and the isoparametric plane strain elements with eight nodes are used. The shrinkage of EMC resulting from the cure is ignored due to its minor effect on the warpage. The material properties of the adhesive, the chip and the lead frame for TSOP are shown in Table 1.

Under the assumption of elastic behavior for the components of TSOP, the material properties at room temperature are used for the chip as well as the adhesive,

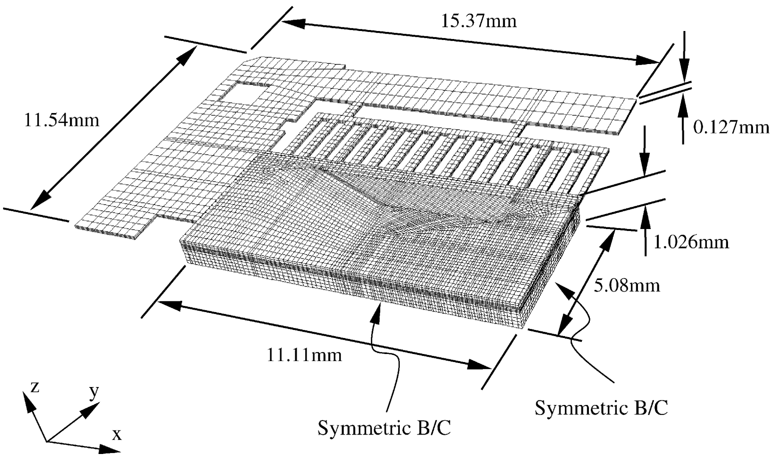

Fig. 5. The size and mesh configuration of TSOP Type I after the molding process and its symmetry B/C.

Table 1
The material properties for the components of TSOP

| | Epoxy (adhesive) | Si (chip) | Alloy 42 (L/F) |
|---|---|---|---|
| Young's modulus (GPa) | 8.8 | 170 | 130 |
| Poisson's ratio | 0.25 | 0.3 | 0.27 |
| CTE (ppm/°C) | 25 | 3 | 4.3 |

and those at the molding temperature are used for EMC. Particularly, the lead frame is assumed that it follows the Prandtl–Reuss equations for the incremental plasticity theory of the isotropic-hardening materials and the calculation of the equations is processed with a power-law hardening rule of the form [9,10]:

$$\frac{\bar{\varepsilon}^{\mathrm{p}}}{\varepsilon_{\mathrm{Y}}} = \alpha\left(\frac{\bar{\sigma}}{\sigma_{\mathrm{Y}}}\right)^{m} \qquad (2)$$

here $\sigma_{\mathrm{Y}}$ is the uniaxial yield stress, which is set to be $\sigma_{\mathrm{Y}} = 634$ MPa for the lead frame, $\bar{\varepsilon}^{\mathrm{p}}$ is the plastic equivalent strain, and $\varepsilon_{\mathrm{Y}} = \sigma_{\mathrm{Y}}/E$ is a reference strain component; $\bar{\sigma}$ is the Mises stress, $\alpha$ is a non-dimensional material constant and $m$ is the power-law hardening exponent. For the numerical computation, $\alpha = 1$ and $m = 12$ are chosen.

Because the warpage begins at the end of the molding process, the temperature boundary condition for this analysis is determined by the cooling down process from the molding temperature, 185 °C to the room temperature, 25 °C.

## 5. Measurement of the warpage in TSOP

The manual measurement system, Profile Project V-24B, is generally used in the actual field of electronic packaging because of its low price and easy handling. The accuracy of the system, however, is not well verified so far. To clarify the usefulness of the warpage values measured by the Profile Project, the accurate measure-

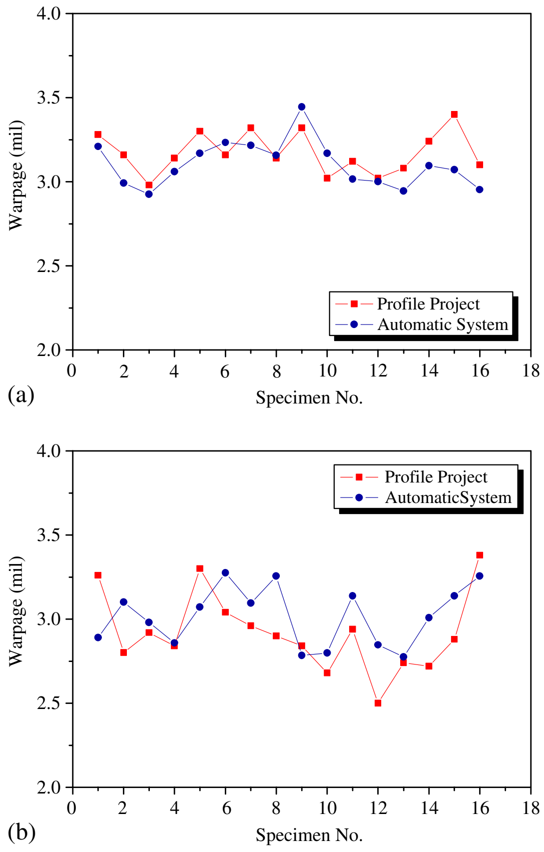

Fig. 6. The comparison between the measuring methods for the warpage of (a) TSOP Type I and (b) TSOP Type II.

ment using automatic measuring system, NEXIV VMR-6555, is carried out and both two results are compared with each other (see Fig. 6).

Even though the warpage values measured by the Profile Project may contain a lot of operating errors in the middle of measuring, it is found that the trend and the magnitude of both warpage values show a good agreement with each other. Therefore, it is helpful to utilize the Profile Project for measuring the warpage in TSOP.

## 6. Results and discussion

The obtained warpage configuration of TSOP Type I is represented in Fig. 7(a) and the considering surface for extracting the warpage value is shown in Fig. 7(b). The computed warpage results of TSOP Type II with respect to the two different degrees of reaction rate of EMC are shown in Fig. 8. From these results, it is found that the lower degree of reaction rate produces the higher warpage value. The degree of reaction rate thus has an important effect on the warpage result.

The warpage data measured with 16 specimens using the automatic measuring system are represented in Fig. 9. The deviation of the measured warpage data stems from the problems in the actual packaging process, i.e., the chip shifting and/or tilting during the die attach and the mold injection process, and the structural variations

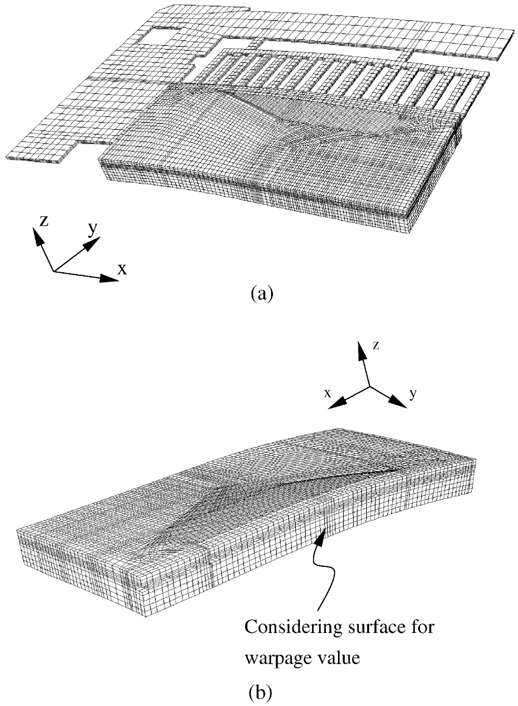

Fig. 7. (a) The warpage configuration of TSOP Type I and (b) the surface of consideration for extracting the warpage values.

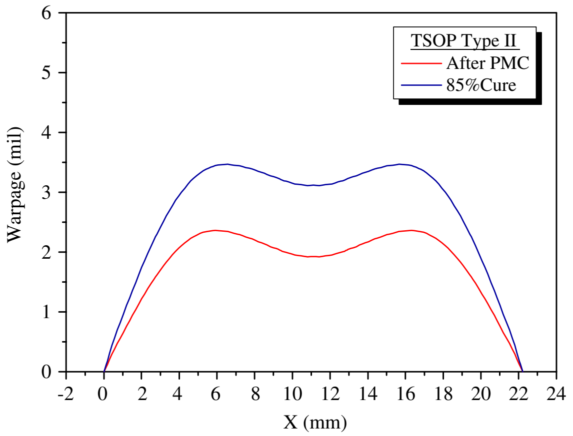

Fig. 8. The computed warpage results with respect to the two different degrees of reaction rate of EMC.

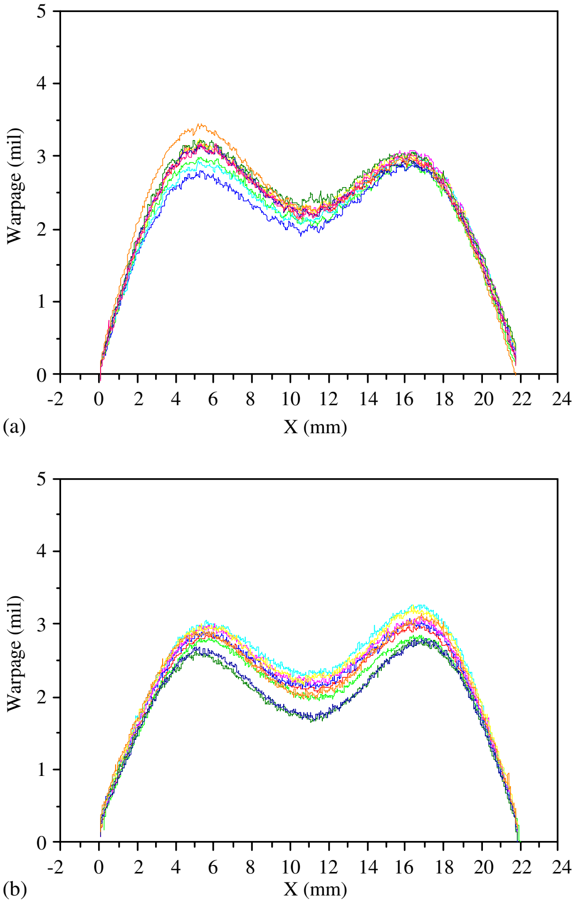

Fig. 9. The measured warpage results for (a) TSOP Type I and (b) TSOP Type II utilizing the automatic measurement system.

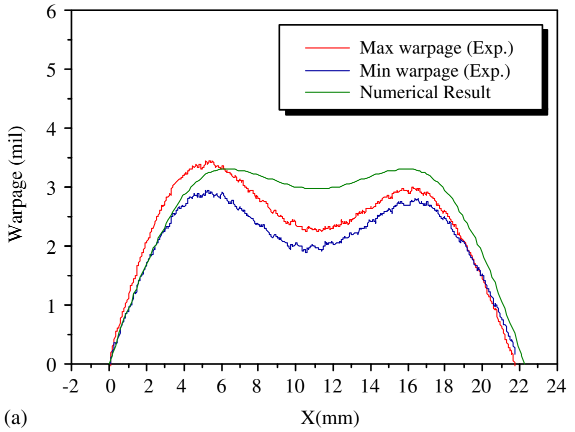

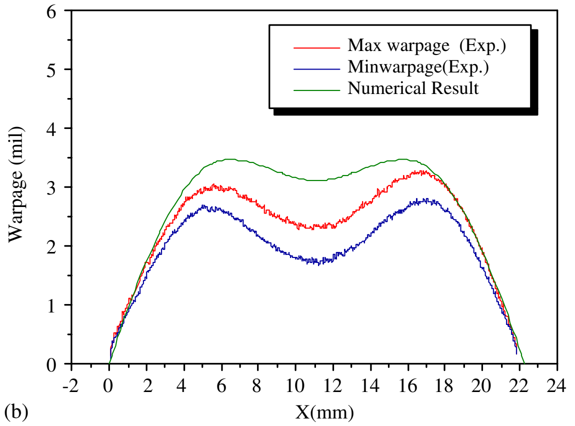

Fig. 10. The comparison between the measured warpage results and the computed ones of (a) TSOP Type I and (b) TSOP Type II.

of each component of TSOP. Moreover, the asymmetric results between the left and the right side from the center of the *x*-coordinate in Fig. 9 stem from the structural asymmetry of the lead frame.

The computed warpage values are compared with the measured ones obtained from the automatic measuring system in Fig. 10. It is shown that the computed ones of both two types of TSOP are higher than the measured ones. Therefore, the computed warpage results can be used to optimize both the material properties of EMC and the geometric structure of each component for TSOP including the concept of the safety factor.

## 7. Concluding remarks

For the numerical analysis of the warpage problem in TSOP, the material properties of EMC depending on the temperature and the degree of reaction rate is measured. Particularly, the material properties at the molding temperature and the degree of reaction rate at the end of the molding process of EMC are used for the computation. The cooling down process from the molding temperature to the room temperature is determined as the external loading to obtain the overestimated warpage results comparing with the actual ones.

Finally, the accurate measurement of the warpage using automatic measuring system, NEXIV VMR-6555, is completed to compare the measured results with the computed ones. From these results, it is found that the numerical analysis gives the higher warpage values than the measured ones. Therefore, the numerical analysis in this study can be easily and conveniently applied to the practical design for the reliable electronic package.

## Acknowledgements

I. Jeon thanks to Mr. Chanki Hwang of Hynix Semiconductor Inc. and Mr. Sangjoon Park of Shinhan Scientific Co. Ltd. for their technical supports. Prof. Beomjoon Kim of University of Tokyo and Dr. Hyon-Jeong Lee are also acknowledged for valuable and helpful advices.

## References

[1] Jong WR, Chang ML. The analytical models for the warpage of integrated circuit devices. ANTEC 99 1999: 1525–9.
[2] Oda J, Sakamoto J. Application of FEM for multiple laminated structure in electronic packaging. Finite Elements Anal Des 1998;30:147–62.
[3] Hamzehdoost A, Yip L. Package warpage evaluation for high performance PQFP. Electronic Components and Technology Conference 45th, 1995. p. 229–33.
[4] Miyake K, Yoshida T, Baik HG, Park SW. Viscoelastic warpage analysis of surface mount package. ASME J Electron Packaging 2001;123:101–4.
[5] Dickson TS, Matthew MF. Warpage of plastic IC packages as a function of processing condition. ASME J Electron Packaging 2001;123:268–72.
[6] Nakmur S, Hasebe A, Serizawa K. Thermo-viscoelastic analysis of warp deformation for resin and metal laminated substrate. 6th MES 95, 1995.
[7] Beom HG, Jeong KM. Evaluation of thermal deformation in electronic packages. KSME Int J 2000;14(2):251–60.
[8] Vyazovkin S, Sbirrazzuoli N. Kinetic method to study isothermal and nonisothermal epoxy-anhydride cure. Macromol Chem Phys 1999;200(10):2294–304.
[9] Jeon I, Im S. The role of higher order eigenfields in elastic-plastic crack. J Mech Phys Solids 2001;49:2789–818.
[10] Jeon I, Lee Y, Im S. Higher order eigenfields in Mode II cracks under elastic–plastic deformation. KSME Int J 2003;17(2):254–68.